

# Small-x Asymptotics of the Quark Helicity Distribution

**Matthew D. Sievert**

with Yuri Kovchegov

and Daniel Pitonyak

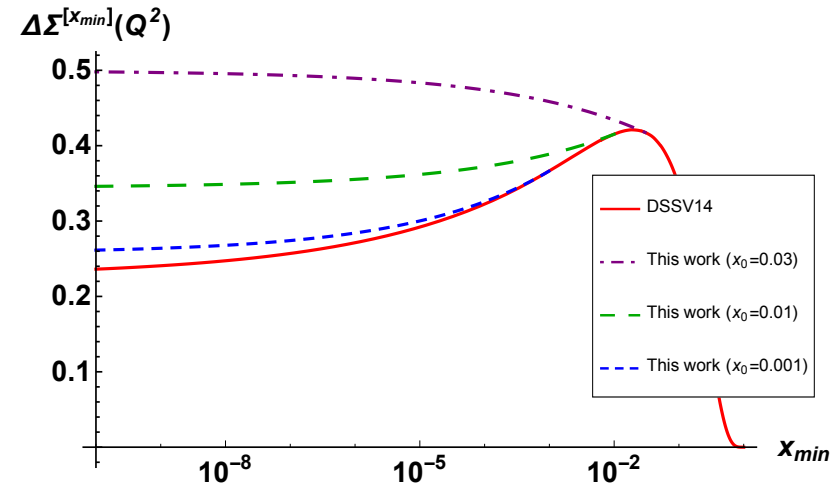
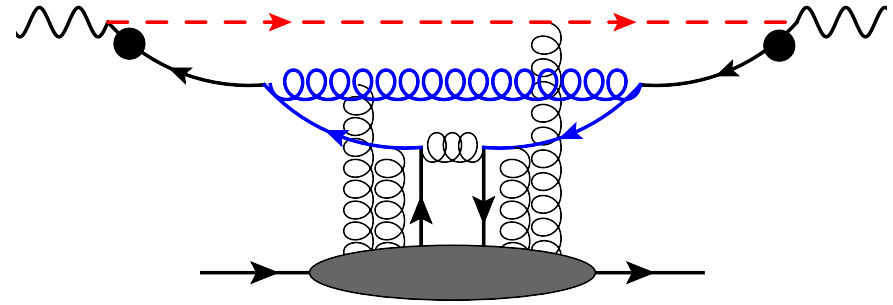


**POETIC 7**, Temple University

Tues. Nov. 15, 2016

# Overview: The Main Message

- Helicity PDF's obey novel, intricate small- $x$  quantum evolution equations.
- Small- $x$  evolution leads to a potentially sizeable contribution to the proton spin.



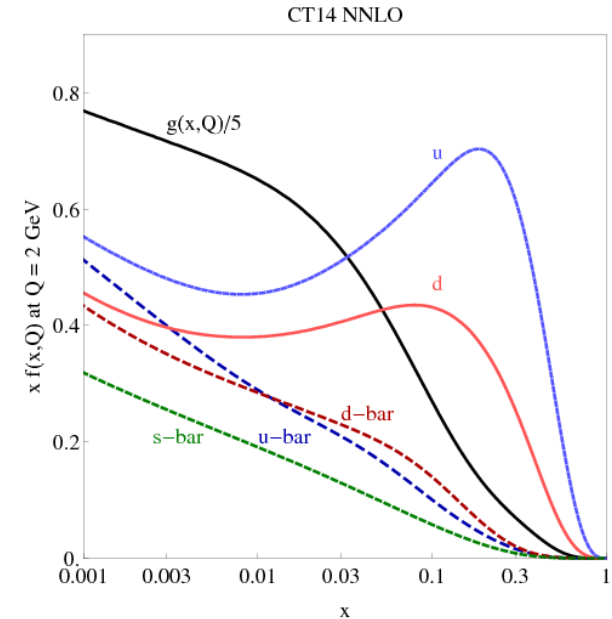
Yuri V. Kovchegov, Daniel Pitonyak, **M.S.**, 1610.06197, submitted to PRD

Yuri V. Kovchegov, Daniel Pitonyak, **M.S.**, 1610.06188, submitted to PRL

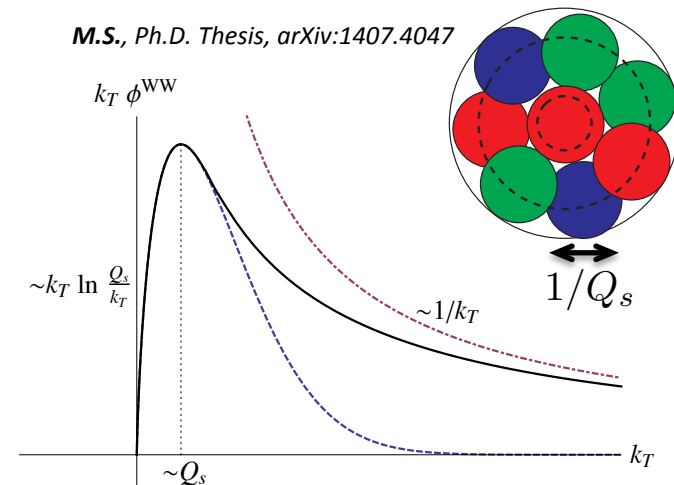
# Motivation: The Small-x Limit of PDF's

- Unpolarized PDF's show a **power-law growth** of gluons and sea quarks at **small x** due to (BFKL) quantum evolution.
- The cascade of small-x gluons **drives up the color-charge density**, enhancing multiple scattering.
- The high-density limit is characterized by the **saturation** of the gluon distribution.

Dulat et al., Phys. Rev. **D93** (2016) no.3 033006



M.S., Ph.D. Thesis, arXiv:1407.4047



# Motivation: Helicity PDF's at Small x

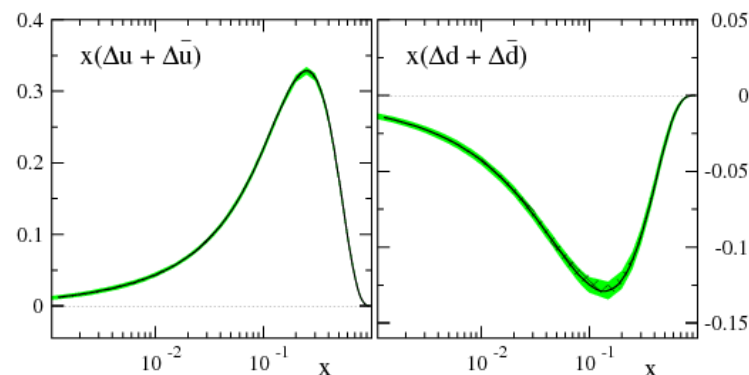
- In contrast, helicity PDF's are suppressed with power-law tails.
- The small-x evolution of helicity PDF's was studied by BER, predicting a growth at small x

*Bartels, Ermolaev, and Ryskin, Z. Phys. C72 (1996) 627*

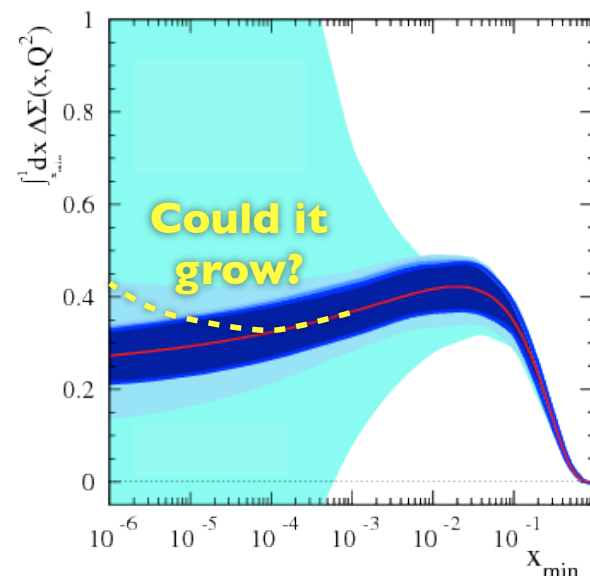
$$x \Delta q \sim \left(\frac{1}{x}\right)^{0.2} \quad \text{for} \quad Q^2 = 10 \text{ GeV}^2$$

- Could the small-x region make an important contribution to the proton spin?
- Could saturation physics be relevant?

*de Florian et al., Phys. Rev. D80 (2009) 034030*



*adapted from Aschenauer et al., Phys. Rev. D92 (2015) no.9 094030*





# Polarized DIS at Small x

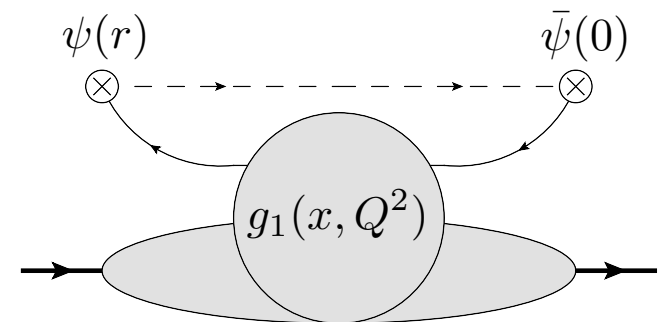
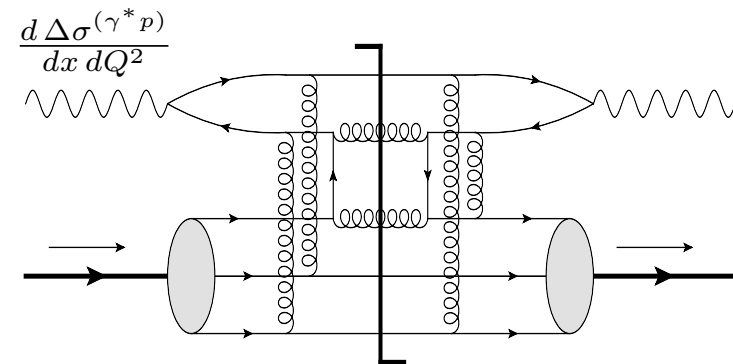
- In DIS at small x, **quark dipole scattering dominates** over quark “knockout”.

- PDF's at small x are described by **dipole scattering amplitudes**.

$$g_1(x, Q^2) = \int dr^- e^{ixp^+ r^-} \langle pS | \bar{\psi}(0) \frac{\gamma^+ \gamma^5}{2} \psi(r) | pS \rangle$$

- Polarized PDF's at small x are described by **polarized dipole scattering amplitudes**.

$$V_{x\perp}(\sigma) = V_{x\perp} + \sigma V_{x\perp}^{pol}$$



$$V_{x\perp} = \mathcal{P} \exp \left[ ig \int dx^+ \hat{A}^-(x^+, 0^-, x_\perp) \right]$$

$$V_{x\perp}^{pol} \neq \mathcal{P} \exp \left[ ig \int dx^+ \hat{A}^-(x^+, 0^-, x_\perp) \right]$$

# The Polarized Dipole Amplitude

- Calculate the **polarized dipole amplitude** by relating it to a **dipole cross-section**.
- Explicitly **scale out energy suppression** of initial conditions:

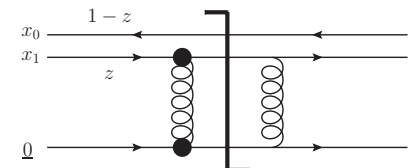
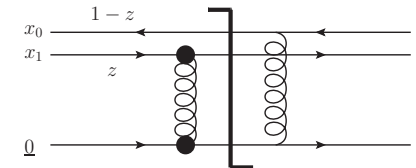
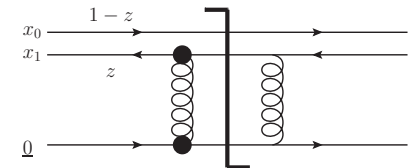
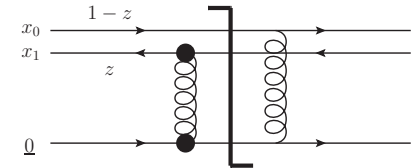
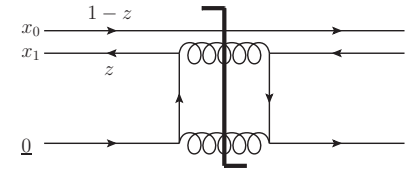
$$G_{10} \equiv \frac{1}{2N_c} \langle\langle \text{Tr}[V_0 V_1^{pol\dagger} + V_1^{pol} V_0^\dagger] \rangle\rangle$$

$$= -\boxed{\frac{zs}{2}} \left[ \boxed{\frac{d\sigma}{d^2b}}(q_0^{unp}, \Delta\bar{q}_1) + \boxed{\frac{d\sigma}{d^2b}}(\Delta q_1, \bar{q}_0^{unp}) \right]$$

- Calculate the **Born initial conditions** to quantum evolution.

$$\vec{x}_{\perp,ij} \equiv \vec{x}_{\perp,i} - \vec{x}_{\perp,j}$$

$$G^{(0)}(x_{10}^2, zs) = \frac{\alpha_s^2 C_F \pi}{N_c} [C_F \ln \frac{zs}{\Lambda^2} - 2 \ln(zs x_{10}^2)]$$



# Origins of Helicity Evolution

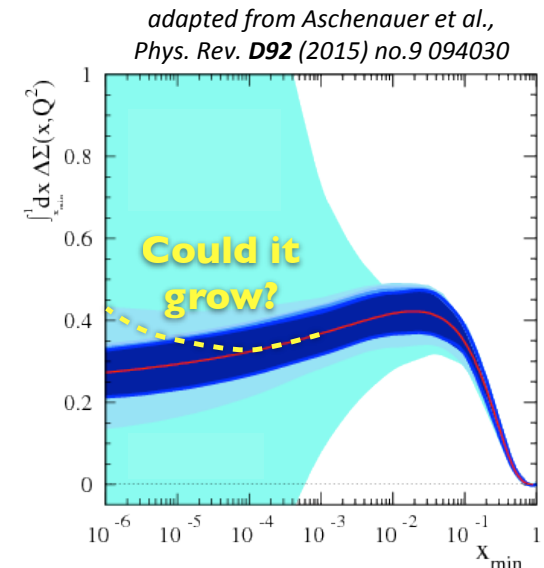
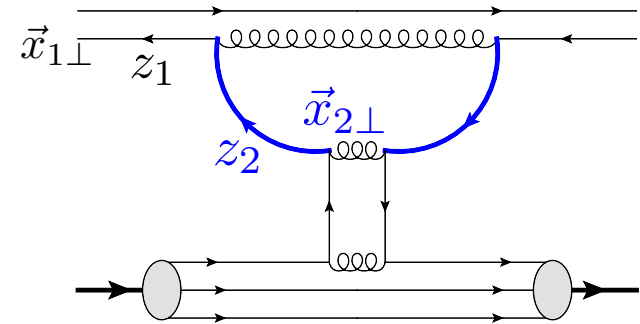
- Helicity evolution is driven by **parton splitting functions** which transfer spin to small  $x$ .

$$\underbrace{\langle V_1^{pol \dagger}(z_1) \rangle}_{\sim \frac{1}{z_1 s}} \sim \int \frac{dz_2}{z_2} \int d^2 x_2 \left( \frac{\alpha_s C_F}{2\pi^2} \frac{z_2}{z_1} \frac{1}{x_{21}^2} \right) \underbrace{\langle V_2^{pol \dagger}(z_2) \rangle}_{\sim \frac{1}{z_2 s}}$$

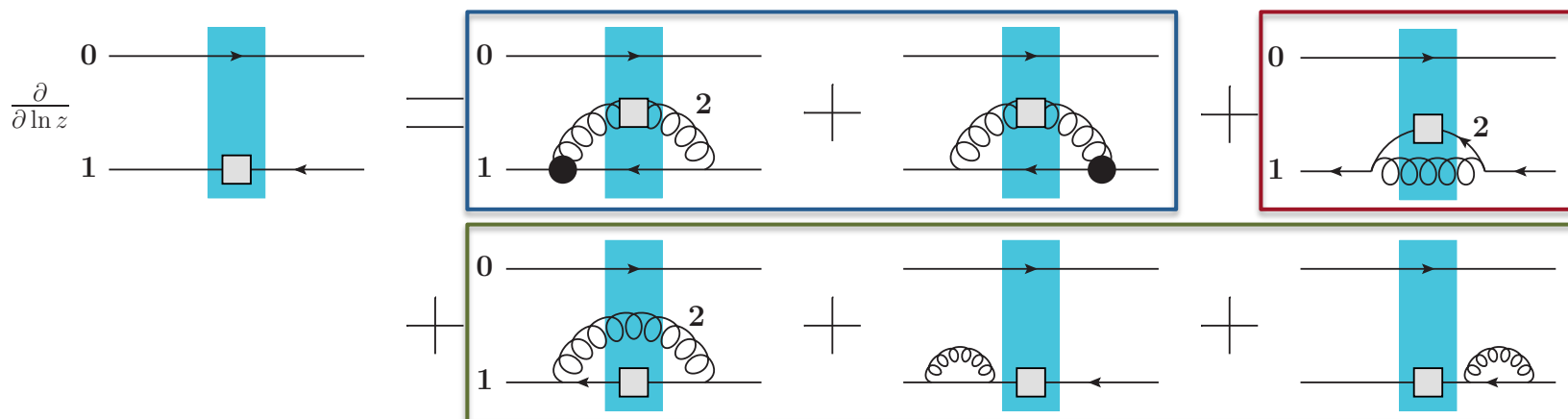
$$G_{10}(z_1) \sim \boxed{\frac{\alpha_s C_F}{2\pi} \int \frac{dz_2}{z_2} \int \frac{dx_{21}^2}{x_{21}^2}} G_{21}(z_2)$$

- Helicity evolution is **double logarithmic**, stronger than unpolarized evolution
- Can strong quantum evolution **reduce or offset the suppression** of helicity at small  $x$ ?

$$\alpha_s \ln^2 \frac{1}{x} \sim 1$$

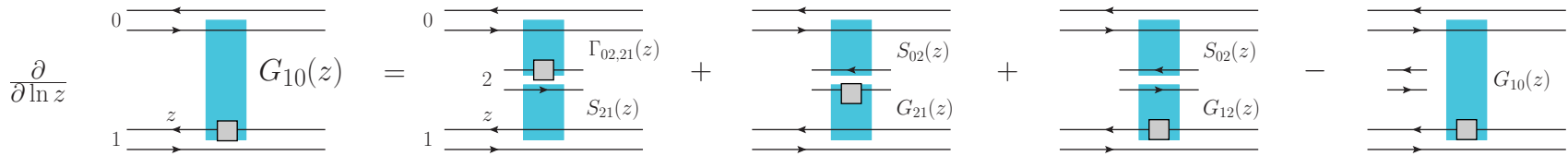


# Helicity Evolution: The Bottom Line



- Soft polarized gluon splitting:  $\theta(x_{10}^2 - x_{21}^2)$
- Soft polarized quark splitting:  $\theta(x_{10}^2 z - x_{21}^2 z')$  Infrared phase space!
- Soft unpolarized gluon splitting:  $\theta(x_{10}^2 - x_{21}^2)$

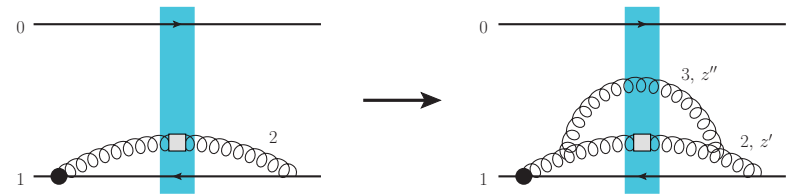
# The Need for Large-Nc Limit



- Helicity evolution leads to an **infinite hierarchy** of operators
- The **large-Nc limit closes the hierarchy** but neglects quarks
- But due to competing phase spaces, **not all dipoles are independent!**

$$Tr[V_0 V_1^{pol \dagger}] \rightarrow \begin{cases} Tr[t^b V_0 t^a V_1^\dagger] (U_2^{pol})^{ba} \\ Tr[V_0 V_1^\dagger] Tr[V_1 V_2^{pol \dagger}] \\ Tr[V_0 V_2^\dagger] Tr[V_2 V_1^{pol \dagger}] \end{cases}$$

$$Tr[V_0 V_1^{pol \dagger}] \rightarrow Tr[V_0 V_1^{pol \dagger}]$$



*Dependence on a neighbor dipole's size!*

$$x_{32}^2 z'' \ll x_{21}^2 z' \quad \text{vs.} \quad x_{32} \ll x_{02}^2$$

# The Large-Nc Equations

$$\underline{G(x_{10}^2, z)} = G^{(0)}(x_{10}^2, z) + \frac{\alpha_s N_c}{2\pi} \int_{\frac{1}{x_{10}^2 s}}^z \frac{dz'}{z'} \int_{\frac{1}{z' s}}^{x_{10}^2} \frac{dx_{21}^2}{x_{21}^2} [\underline{\Gamma(x_{10}^2, x_{21}^2, z')}] + \underline{3G(x_{21}^2, z')}$$

$$\underline{\Gamma(x_{10}^2, x_{21}^2, z')} = G^{(0)}(x_{10}^2, z') + \frac{\alpha_s N_c}{2\pi} \int_{\frac{1}{x_{10}^2 s}}^{z'} \frac{dz''}{z''} \int_{\frac{1}{z'' s}}^{\min[x_{10}^2, x_{21}^2 \frac{z'}{z''}]} \frac{dx_{32}^2}{x_{32}^2} [\underline{\Gamma(x_{10}^2, x_{32}^2, z'')}] + \underline{3G(x_{32}^2, z'')}$$

- System of equations for the **dipole** + “neighbor dipole”
- Neighbor dipole differs due to **competing phase space constraints**
- **Initial conditions:**  $G^{(0)}(x_{10}^2, zs) = \frac{\alpha_s^2 C_F \pi}{N_c} [C_F \ln \frac{zs}{\Lambda^2} - 2 \ln(zs x_{10}^2)]$

# Attempting an Analytical Solution

$$G(s_{10}, \eta) = G^{(0)}(s_{10}, \eta) + \int_{s_{10}}^{\eta} d\eta' \int_{s_{10}}^{\eta'} ds_{21} [\Gamma(s_{10}, s_{21}, \eta') + 3G(s_{21}, \eta')]$$

$$\Gamma(s_{10}, s_{21}, \eta') = G^{(0)}(s_{10}, \eta') + \int_{s_{10}}^{\eta'} d\eta'' \int_{\max[s_{10}, s_{21} + \eta'' - \eta']}^{\eta'} ds_{32} [\Gamma(s_{10}, s_{32}, \eta'') + 3G(s_{32}, \eta'')]$$

- Change to **rescaled logarithmic variables**
- Standard technique: **Laplace/Mellin transform + saddle point approximation**

$$s_{ij} \equiv \sqrt{\frac{\alpha_s N_c}{2\pi}} \ln \frac{1}{x_{ij}^2 \Lambda^2}$$

$$\eta^{(\prime, \prime\prime)} \equiv \sqrt{\frac{\alpha_s N_c}{2\pi}} \ln \frac{z^{(\prime, \prime\prime)}}{\Lambda^2/s}$$

$$G(s_{10}, \eta) = \int \frac{d\omega}{2\pi i} e^{\omega\eta} \int \frac{d\lambda}{2\pi i} e^{\lambda s_{10}} G_{\omega\lambda} \longleftrightarrow G_{\omega\lambda} = \int_0^\infty ds_{10} e^{-\lambda s_{10}} \int_0^\infty d\eta e^{-\omega\eta} G(s_{10}, \eta)$$

- **Fails** because the **neighbor dipole couples the arguments** in Mellin space!

# Resorting to a Numerical Solution

- Resort to discretizing on a grid and solving numerically

$$\begin{aligned} \eta_i &= i \Delta\eta \\ s_j &= j \Delta\eta \end{aligned} \quad i, j = 0 \dots N \quad N = \frac{\eta_{max}}{\Delta\eta}$$

- Choose endpoints to allow an iterative solution

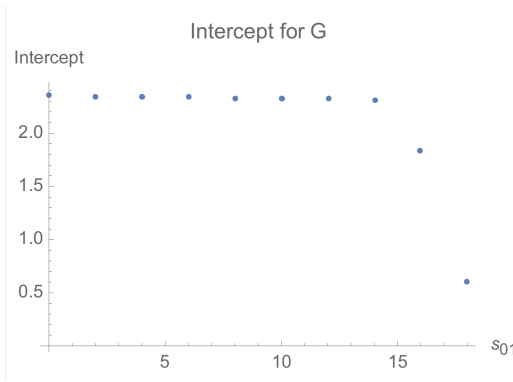
$$G_{ij} = G_{ij}^{(0)} + \Delta\eta^2 \sum_{j'=i}^{j-1} \sum_{i'=i}^{j'} [\Gamma_{ii'j'} + 3G_{i'j'}]$$

$$\Gamma_{ikj} = G_{ij}^{(0)} + \Delta\eta^2 \sum_{j'=i}^{j-1} \sum_{i'=max[i, k+j'-j]}^{j'} [\Gamma_{ii'j'} + 3G_{i'j'}]$$

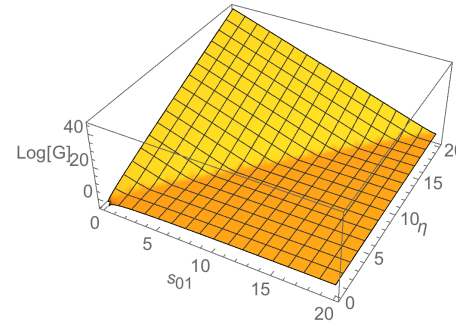
- For fixed grid parameters  $(\Delta\eta, \eta_{max})$ , we can calculate the polarized dipole starting from the initial conditions at  $\eta = 0$ .



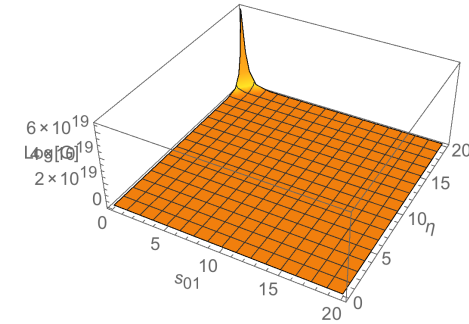
# Extracting the Small-x Asymptotics



Numerical Solution  $G(s_{01}, \eta)$ , physical only for  $\eta > s_{01}$



Numerical Solution  $G(s_{01}, \eta)$ , physical only for  $\eta > s_{01}$



- Evolve in  $\eta$  until the **asymptotic power-law behavior** sets in.
- **Fit the slope** of  $\ln G$  in the upper 25% of the  $\eta$  range to **extract the intercept** (power)  $\alpha_h$ .
- For a **given set of grid parameters**, we obtain the intercept

$$G(zs) \sim \exp \left[ \sqrt{\frac{2\pi}{\alpha_s N_c}} \alpha_h \eta \right] \sim (zs)^{\alpha_h}$$



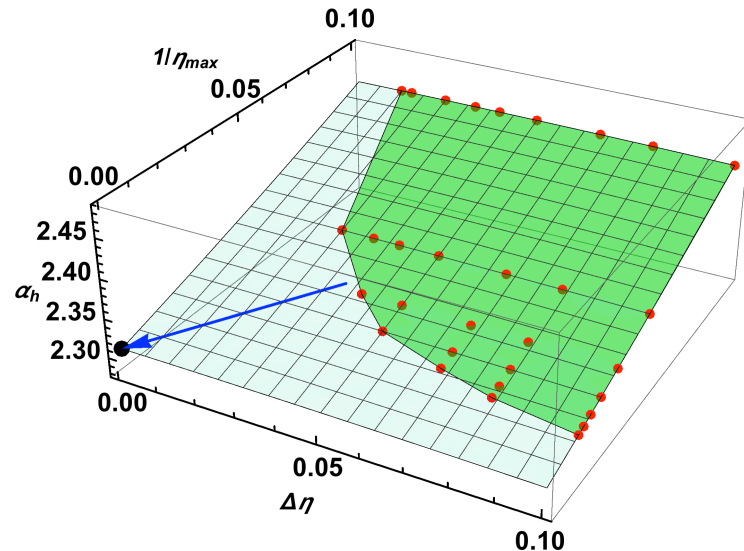
$$\alpha_h = \sqrt{\frac{\alpha_s N_c}{2\pi}} \frac{\partial}{\partial \eta} \ln G$$



$$\alpha_h(\Delta\eta, \eta_{max})$$

# Extrapolating to the Continuum

- We can scan the grid parameter space up to a computational limit on the grid size:  $N = \frac{\eta_{max}}{\Delta\eta} = 500$
- The physical point is  $(\Delta\eta, \eta_{max}) \rightarrow (0, \infty)$
- Fit all “data points” to a continuous function  $\alpha_h(\Delta\eta, \eta_{max})$
- Use an AIC-weighted average to extrapolate to the physical point.



$$\alpha_h(\Delta\eta, \eta_{max}) = A(\Delta\eta) + B(\Delta\eta)^2 + C\left(\frac{1}{\eta_{max}}\right) + D\left(\frac{1}{\eta_{max}}\right)^2$$

⋮

$$\alpha_h(\Delta\eta, \eta_{max}) = A(\Delta\eta)^B + C(\Delta\eta)^D + E\left(\Delta\eta \times \frac{1}{\eta_{max}}\right)^F$$

Akaike, *IEEE Transactions on Automatic Control*, **19** (6) 716 (1974)

# Our Result: The Small-x Tail

$$\begin{aligned}\Delta q(x, Q^2) &\sim \left(\frac{1}{x}\right)^{\alpha_h} \\ g_1(x, Q^2) &\sim \left(\frac{1}{x}\right)^{\alpha_h} \\ \Delta\Sigma(Q^2) &\equiv \int_0^1 dx \Delta q(x, Q^2) \sim \int_0^1 dx \left(\frac{1}{x}\right)^{\alpha_h}\end{aligned}$$

Intercept

- Our results (flavor-singlet , pure glue, large- $N_c$ ):
- Fixed coupling:
- First QCD constraint on the small-x limit of the helicity PDF's!
- Flavor non-singlet case does not couple to gluons (40% smaller)

$$\alpha_h = 2.31 \sqrt{\frac{\alpha_s N_c}{2\pi}}$$

$Q^2 = 3 \text{ GeV}^2$	$Q^2 = 10 \text{ GeV}^2$
$\alpha_h = 0.936$	$\alpha_h = 0.797$

$$\alpha_h^{NS} = \sqrt{2} \sqrt{\frac{\alpha_s N_c}{2\pi}}$$

# A Surprising Discrepancy

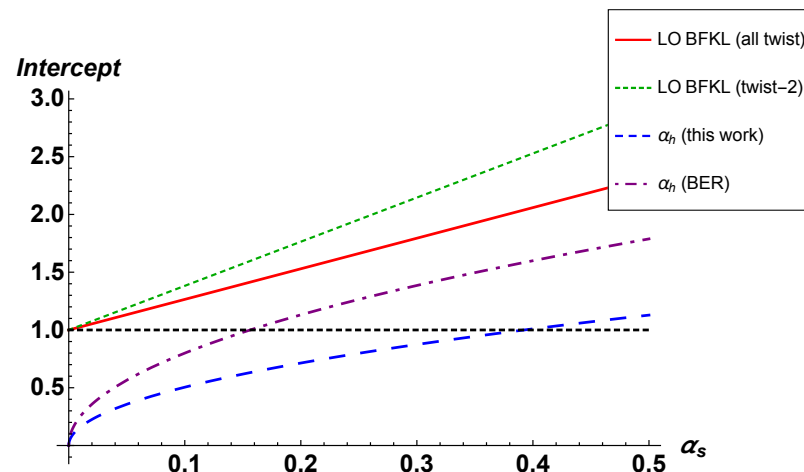
- Our results (pure glue, large- $N_c$ ):

$$\alpha_h = 2.31 \sqrt{\frac{\alpha_s N_c}{2\pi}}$$

*Bartels, Ermolaev, and Ryskin, Z. Phys. C72 (1996) 627*

- BER (pure glue,  $N_c$ -independent):

$$\alpha_h = 3.66 \sqrt{\frac{\alpha_s N_c}{2\pi}}$$



for  $Q^2 = 10 \text{ GeV}^2$

- Our intercept is 35% smaller than BER and generally integrable as  $x \rightarrow 0$ .

$$\Delta\Sigma = \int_0^1 dx \Delta q \sim \int_0^1 dx \left(\frac{1}{x}\right)^{0.80}$$

Us: converges!

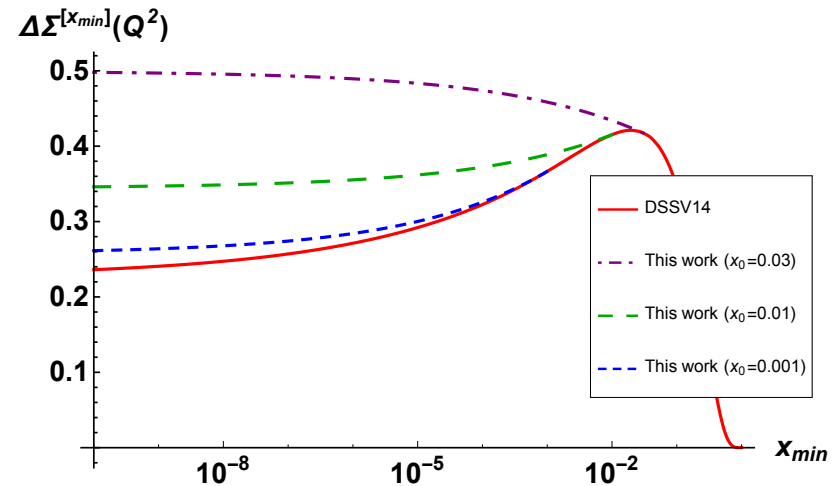
- A similar decrease is seen from the all-twist to leading-twist BFKL intercept....

$$\Delta\Sigma = \int_0^1 dx \Delta q \sim \int_0^1 dx \left(\frac{1}{x}\right)^{1.26}$$

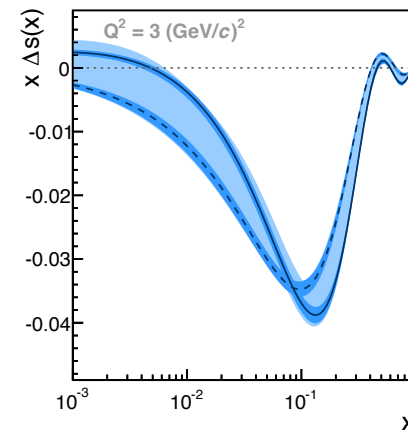
BER: diverges!

# Implications for the Proton Spin Puzzle

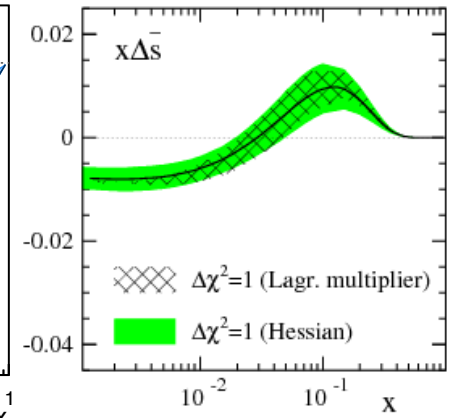
- Our intercept can be combined with PDF fits to estimate the small- $x$  contribution to the proton spin.
- The small- $x$  tail can make a **potentially large contribution!**
- But... depends strongly on the **approach to small  $x$** :
  - Onset of small- $x$  behavior...
  - Assumptions about **flavor symmetry** in the sea...
  - Strange quark fragmentation functions...



Adolph et al., Phys. Lett. **B753**  
(2016) 18

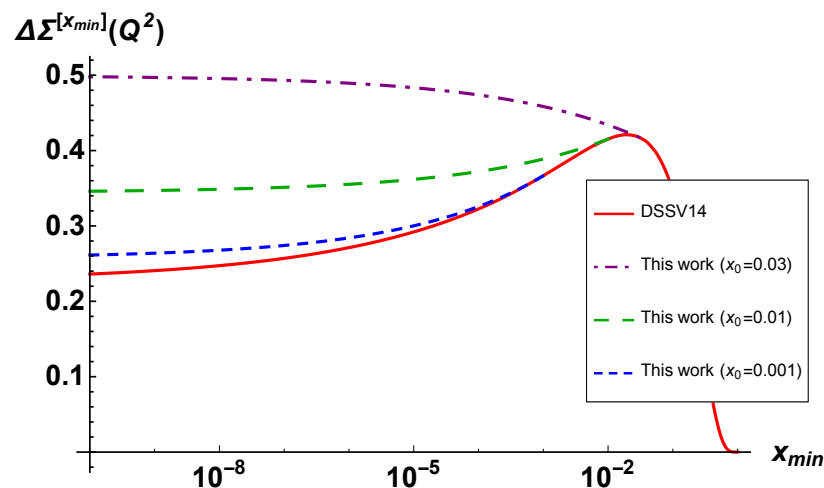
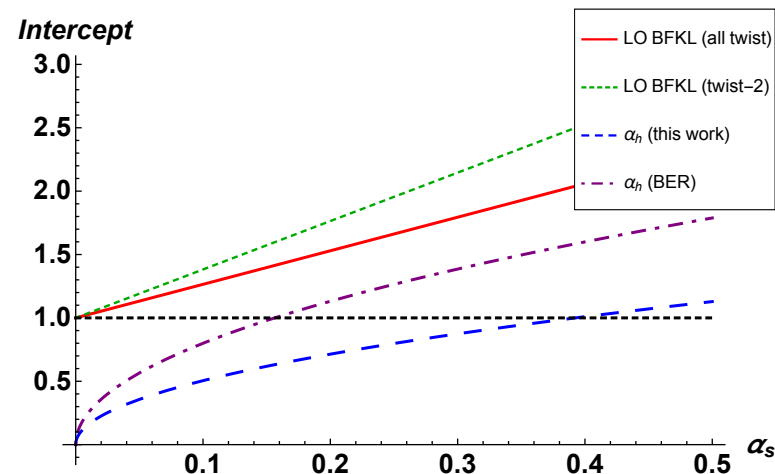


de Florian et al., Phys. Rev. **D80**  
(2009) 034030



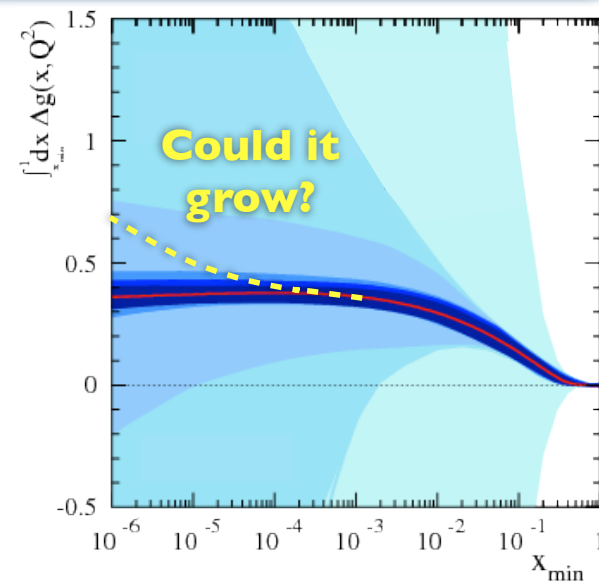
# Conclusions

- Our numerical solution gives the **first QCD constraints** on the **small- $x$  asymptotics** of helicity PDF's.
- The **enhancement** we find at small  $x$  is **35% smaller** than in the literature.
- Can make a **substantial contribution to the proton spin puzzle**.
- This result **needs to be incorporated** from the ground level in the **next-generation PDF fits**.



# Outlook: Future Directions

- Show that the **same intercept** describes the gluon helicity PDF at small  $x$ . (*in progress*)
- Include **quarks** by taking the **large  $N_c + N_f$  limit**. (*cumbersome but straightforward*)
- **Leading-log** evolution and **saturation** corrections (*hard...*)
- **Finite- $N_c$**  corrections (*hard...*)
- **Other polarization observables** (*the sky's the limit!*)



		Quark Polarization		
		Un-Polarized (U)	Longitudinally Polarized (L)	Transversely Polarized (T)
Nucleon Polarization	U	$f_1 = \odot$		$h_1^\perp = \uparrow - \downarrow$ Boer-Mulders
	L		$g_{1L} = \rightarrow - \leftarrow$ Helicity	$h_{1L}^\perp = \rightarrow - \leftarrow$
	T	$f_{1T}^\perp = \uparrow - \downarrow$ Sivers	$g_{1T}^\perp = \uparrow - \leftarrow$	$h_1 = \uparrow - \downarrow$ Transversity $h_{1T}^\perp = \rightarrow - \leftarrow$

# Backup Slides: The Disagreement with BER

*Bartels et al., Z. Phys. **C72** (1996) 627*



# What Do BJR Do?

$$\mu^2 \frac{\partial}{\partial \mu^2} \left( \text{Diagram 1} \right) = \mu^2 \frac{\partial}{\partial \mu^2} \left( \text{Diagram 2} + \text{Diagram 3} \right) + \mu^2 \frac{\partial}{\partial \mu^2} \left( \text{Diagram 4} + \text{Diagram 5} \right)$$

$$\mu^2 \frac{\partial}{\partial \mu^2} \left( \text{Diagram 6} \right) = \mu^2 \frac{\partial}{\partial \mu^2} \left( \text{Diagram 7} \right) + \mu^2 \frac{\partial}{\partial \mu^2} \left( \text{Diagram 8} \right) + \mu^2 \frac{\partial}{\partial \mu^2} \left( \text{Diagram 9} \right)$$

- Attempt to re-sum mixed logarithms of  $x$  and  $Q^2$ .  

$$(\alpha_s)^n [b_n (\ln(1/x))^{2n} + b_{n-1} (\ln(1/x))^{2n-1} \ln(Q^2/\mu^2) + \dots + b_0 (\ln(1/x))^n (\ln(Q^2/\mu^2))^n]$$
- They also have both ladder and non-ladder gluons (the primary source of our complexity)
- Their calculation uses Feynman gauge (we use light-cone gauge).

# What are BER's Equations?

- Transform the spin-dependent part of the hadronic tensor to Mellin space:

$$T_3 = \int_{-i\infty}^{i\infty} \frac{d\omega}{2\pi i} \left(\frac{s}{\mu^2}\right)^\omega \xi(\omega) R(\omega, y)$$

- Write down “infrared evolution equations” in Mellin space:

$$\left(\omega + \frac{\partial}{\partial y}\right) R = \frac{1}{8\pi^2} F_0 R \quad y = \ln\left(\frac{Q^2}{\mu^2}\right)$$

- Obtained coupled matrix equations which can be solved analytically

$$F_0 = \begin{pmatrix} F_{gg} & F_{qg} \\ F_{gq} & F_{qq} \end{pmatrix} \quad M_0 = \begin{pmatrix} 4C_A & -2T_f \\ 2C_F & C_F \end{pmatrix}$$

$$F_0(\omega) = \frac{g^2}{\omega} M_0 - \frac{g^2}{2\pi^2\omega^2} G_0 F_8(\omega) + \frac{1}{8\pi^2\omega} F_0(\omega)^2$$

$$G_0 = \begin{pmatrix} C_A & 0 \\ 0 & C_F \end{pmatrix} \quad M_8 = \begin{pmatrix} 2C_A & -T_f \\ C_A & -1/2N \end{pmatrix}$$

$$F_8 = \frac{g^2}{\omega} M_8 + \frac{g^2 C_A}{8\pi^2\omega} \frac{d}{d\omega} F_8(\omega) + \frac{1}{8\pi^2\omega} F_8(\omega)^2$$

# BER's Solution

- They obtain an analytic expression, with the intercept determined by the eigenvalues of their matrices.

$$g_1(x, Q^2) = \frac{\omega_s^{3/2}}{8\sqrt{2\pi}} \frac{\frac{2}{\omega_s} + \ln Q^2/\mu^2}{(\ln(1/x))^{3/2}} (\Delta g, \Delta \Sigma) R(\omega_s, y) \left( \frac{1}{x} \right)^{\omega_s} \left( 1 + O\left( \frac{\ln^2 Q^2/\mu^2}{\ln 1/x} \right) \right)$$

- But all the complexity actually only leads to a small effect compared to the ladder graphs.

Ladder only:

$$\omega_s = z_s \sqrt{\alpha_s N_c / 2\pi}$$

$$z_s = 3.45 \quad (n_f = 4)$$

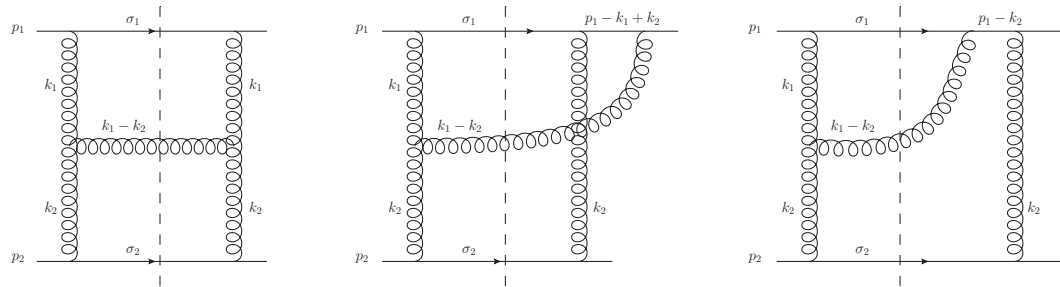
$$z = 3.66 \quad \text{pure glue}$$

$$z_s = 3.81 \quad (n_f = 4)$$

$$z_s = 4 \quad \text{pure glue}$$

- We agree on the ladder part, but we seem to include additional diagrams which lead to a larger effect.

# Diagrammatic Discrepancies



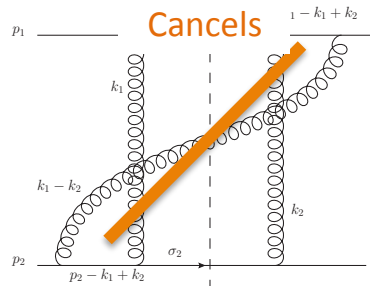
A

B

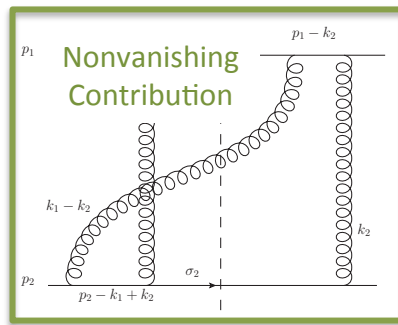
C

Us: All Cancel

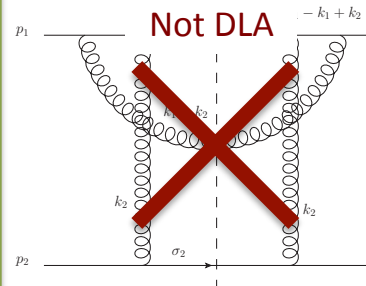
BER: B+C = 0 for  $k_{2T}^2 \gg k_{1T}^2$ ,  
A = nonvanishing contribution



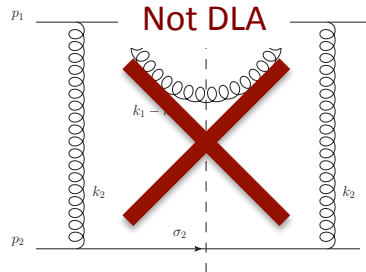
D



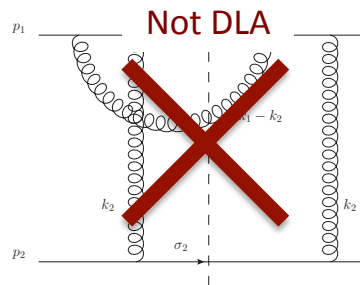
E



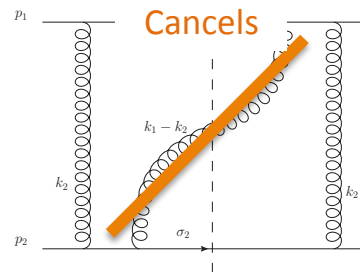
F



G



H



I

Not considered by BER?

# Anomalous Dimensions

- They reproduce the DGLAP anomalous dimensions to NLO (and beyond)...

$$\gamma_S^{(1)} = \left(\frac{\alpha_s}{4\pi}\right)^2 \frac{1}{\omega^3} \begin{pmatrix} 32C_A^2 - 16C_F T_f & -16C_A T_f - 8C_F T_f \\ 16C_A C_F + 8C_F^2 & 4C_F^2 - 16C_F T_f + \frac{8C_F}{N} \end{pmatrix}$$

- We also reproduce the G/G anomalous dimension in the large- $N_c$  limit...

$$\gamma_{S,GG}^{(1)}(\omega) = \left(\frac{\alpha_s}{2\pi}\right)^2 8N_c^2 \frac{1}{\omega^3}$$

- Whatever diagrams they exclude do not miss any leading logarithms of  $Q^2$ ...
- Perhaps our disagreement is over higher-twist corrections? That would explain our 35% smaller intercept....